Solvent entropy contribution to the free energy of protein crystallization

Peter G. Vekilov[a], Angela R. Feeling-Taylor[b], Siu-Tung Yau[c] and Dimiter Petsev[d]

[a]Department of Chemical Engineering, University of Houston, Houston, TX 77204-4004, USA, [b]Department of Anatomy and Structural Biology, Albert Einstein College of Medicine, Bronx, NY 10461, USA, [c]Department of Physics, Hunter College, CUNY, New York, NY 10021, USA, and [d]Center for Microgravity and Materials Research, University of Alabama in Huntsville, Huntsville, AL 35899, USA. E-mail: vekilov@uh.edu

We show with three proteins that trapping and release of the water molecules upon crystallization is a determinant of the crystallization thermodynamics. With HbC, a strong retrograde solubility dependence on temperature yields a high positive enthalpy of 155 kJ mol^{-1}, i.e., crystallization is only possible because of the huge entropy gain of 610 J mol^{-1}K^{-1}, stemming from the release of up to 10 water molecules per protein intermolecular contact. With apoferritin, the enthalpy of crystallization is close to zero. The main component in the crystallization driving force is the entropy gain due to the release upon crystallization of two water molecules bound to one protein molecules in solution. With both proteins, the density of the growth sites imaged by AFM is in excellent agreement with a calculation using the crystallization free energy. With lysozyme, the entropy effect due to the restructuring of the water molecules is negative. This leads to higher solubility.

Keywords: crystallization free energy, solubility, solvent entropy, endothermic crystallization, water molecules

1. Introduction

A major difference between the crystallization of proteins and of small molecules is that the crystals' building blocks are one, two or three orders of magnitude larger than the solvent molecules: water, as well as ions and organic compounds. One consequence is that the solvent fills the voids between the molecules in the crystals (McPherson, 1982). Another consequence is that the solvent is associated with the protein molecules in the dissolved state and the contribution of the solvent association and dissociation can be separated from the overall thermodynamics of the phase transition. As we show here, in many cases these contributions are a significant, and are often the overwhelming part of the thermodynamic balance of crystallization.

Water, the native solvent for proteins and the one from which the formation of their solid phases occurs, is often viewed as an inert medium holding the protein molecules. Although the role of the hydrogen, electrostatic, hydrophobic and other water-mediated interactions in protein folding, binding, function, etc., is well understood (Eaton *et al.*, 1997; Fersht, 1999), the viewpoint of "water inertness" seems to be supported by the evidence that at least some proteins fold correctly and function even in non-aqueous solvents (Rariy & Klibanov, 1997). Along these lines, the chemical nature of water, the dynamics of the interactions between water, protein and the other constituents of the solution are not considered crucial for the phase transitions into which a protein may participate. Here, we illustrate the opposite concept—that zooming in and tracking the water attached to the protein molecules in the solution and in the solid phases (crystal, polymer, amorphous aggregate, etc.) provide insight that may suggest novel means to control the protein phase transitions.

In many of the high-resolution protein structures studied by x-ray or neutron diffraction from crystals, a significant fraction of the water molecules in the channels between the proteins are identifiable. This means that the arrangement of the water molecules around all protein molecules in the crystal is identical. This reproducibility suggests the action of specific forces between the protein surface and the water that leads to structuring of the water around the protein molecules. Similar water structures must exist even when the protein molecule is in the solute state prior to crystallization. Then, as the protein molecules get together to form the new solid phase, these structures must undergo some kind of restructuring: rearrangement, release of some of the associated waters, or trapping of even more water molecules. This restructuring is accompanied by an energy exchange that is an essential part of the enthalpy balance of the phase transition. It is important to realize that the release, trapping and rearrangement of the water also have a significant *entropy* effect. The sign of this effect maybe positive, i.e., entropy is gained which favors the phase transition, or negative, indicating entropy loss, which favors the free protein molecules in the solution. In this sense, the processes of protein crystallization are akin to phenomena underlying hydrophobic attraction that governs many processes in nature (Israelachvili, 1995), including some stages of protein folding (Eaton *et al.*, 1997).

These considerations allow separation of the contribution of the entropy change due to the restructuring of the water shells around the protein molecules $\Delta S^{o}_{\rm solvent}$ from the overall entropy change during crystallization ΔS^{o}. The expression for the standard free energy for crystallization ΔG can then be re-written as

$$\Delta G^{o} = \Delta H^{o} - T\,\Delta S^{o} = \Delta H^{o} - T\,\Delta S^{o}_{\rm protein} - T\,\Delta S^{o}_{\rm solvent}, \qquad (1)$$

where ΔH^{o} is the standard enthalpy for crystallization and may be smaller or greater than 0. $\Delta S^{o}_{\rm protein}$ is the entropy change upon the attachment of the protein molecules to the crystal and contains the balance between the constrained translational and rotational degrees of freedom, and the gain of vibrational entropy due to the newly created bonds at the molecular contacts (Tidor & Karplus, 1994).

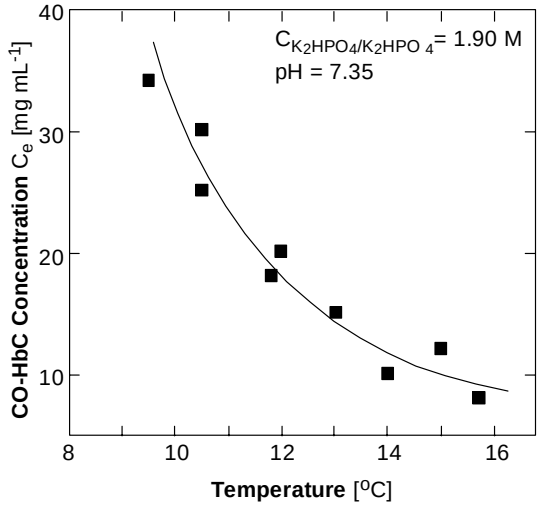

Figure 1
Dependence of solubility C_e of carbomonoxy-hemoglobin C on temperature at conditions indicated in the plot. Points: experimental results; curve: fit to Eq. (4.) using ΔH = 155 kJ/mol.

Generally, the balance between the two is expected to yield $\Delta S^{o}_{protein} < 0$. As discussed above, $\Delta S^{o}_{solvent}$ may be > or < 0.

Below, we discuss three examples from the field of protein crystallization, in which the entropy change due the release or trapping of the water molecules around the protein molecules is a crucial factor in the thermodynamics of the process. In the first two examples, human hemoglobin C, and apoferritin, the entropy gain due to the release of the solvent molecules is the component of the free energy of crystallization that makes it negative and enables the process. In the third case, that of lysozyme, the entropy effect due to the restructuring of the solvent molecules is negative. This reduces the magnitude of the crystallization free energy from the value set by the enthalpy and in this way leads to higher solubility.

2. Human hemoglobin C – positive enthalpy of crystallization

2.1. Enthalpy, entropy and free energy of crystallization

To characterize the thermodynamics of crystallization of this protein in its stable, carbomonoxy (CO) form, the dependence of its solubility of temperature was determined in a solution in 1.9 M phosphate buffer at pH 7.37 (Feeling-Taylor *et al.*, 1999). Typically, at these conditions the crystals of this protein grow to sizes of 0.5-1 mm and are suitable for x-ray diffraction studies.

The solubility of CO-HbC as a function of temperature is plotted in Figure 1. The higher solubility at lower temperature, "retrograde" temperature dependence of solubility (Rosenberger *et al.*, 1993), is similar to the one known for deoxy-HbS (Ross *et al.*, 1977), and has been encountered with many other proteins (McPherson, 1982; 1999).

This retrograde temperature dependence of solubility can be understood in terms of the Gibbs-Helmholtz equation

$$\left(\frac{\partial \ln K_{\rm cryst}}{\partial T}\right)_p = \left[\frac{\partial\left(\Delta G^{\rm o}/{\rm R}T\right)}{\partial T}\right]_p = \frac{\Delta H^{\rm o}}{{\rm R}T^2}, \qquad (2)$$

where $K_{\rm cryst} \equiv \exp(-\Delta G^{\circ}/{\rm R}T)$ is the equilibrium constant for crystallization, T is the absolute temperature, ΔG^{o} is the standard change of Gibbs free energy upon crystallization, R = 8.314 J mol^{-1} K^{-1} is the universal gas constant, and ΔH^{o} is the standard crystallization enthalpy.

The crystallization equilibrium constant $K_{\rm cryst}$ can be represented as (Atkins, 1998)

$$K_{\rm cryst} = a_e^{-1} = \left(\gamma_e \frac{C_e}{C^o}\right)^{-1} \approx \left(\frac{C_e}{C^o}\right)^{-1} \qquad (3)$$

where a_e is the activity of the Hb in solution in equilibrium with the crystals, γ_e and C_e are, respectively, the corresponding activity coefficient and concentration, and C^{o} = 1 mol kg^{-1} is the concentration of the solution in the chosen standard state. The last approximate equality in Eq. (3) is based on the assumption that $\gamma_e \approx 1$, i.e., the solution is close to ideal. To avoid this assumption, we could experimentally evaluate γ at the crystallizing conditions by using its link to the second virial coefficient (Hill, 1963), as we do below for apoferritin and lysozyme. Unfortunately, such determinations are not possible for a crystallizing solution of CO-HbC because of the shifts of the average particle size, indicative of protein aggregation. For an indication of the error introduced by the ideality assumption, we compare it with the deviation from ideality of the osmotic pressure of a solution of deoxy-HbS: at C = 20 mg mL^{-1} it is 5 %, and, at C = 40 mg mL^{-1}, 7 % (Ross & Minton, 1977). We conclude that the ideality assumption may bring about up to 10 % error in the following evaluations.

Combining Eqs. (2) and (3), we get

$$\left[\frac{\partial \ln\left(C_e/C^o\right)}{\partial T}\right]_p = -\frac{\Delta H^{\rm o}}{{\rm R}T^2} \quad . \qquad (4)$$

The data in Figure 1 fit a single exponent with a best-fit value of ΔH^{o} = 155 ± 10 kJ mol^{-1}, with the positive sign of the enthalpy stemming from the negative sign of $(\partial C_e/\partial T)$. Positive crystallization enthalpy, i.e., endothermic crystallization, means that heat is consumed during crystallization. For the process to be thermodynamically permissible, the standard free energy of crystallization ΔG^{o}, defined by Eq. (1), must be negative, i.e., the entropy component $T\,\Delta S^{o} > \Delta H^{o}$.

The data in Figure 1 allow evaluation of ΔG^{o}. Using Eq. (3),

$$\Delta G^{o} = RT\ln a_e \cong RT\ln(C_e/C^{o}). \qquad (5)$$

At T = 16 °C, with C_e = 9 mg mL^{-1} = 0.00014 mol kg^{-1}, ΔG^{o} = –21.3 kJ mol^{-1}. At T = 10 °C, with C_e = 32 mg mL^{-1} = 0.0005 mol kg^{-1} we get ΔG^{o} = –17.9 kJ mol^{-1}. From these and ΔH^{o}, using Eq. (1), we get for both temperatures ΔS^{o} = 610 J mol^{-1} K^{-1}. Note that both ΔH^{o} and ΔS^{o} do not change in the above temperature interval, and all changes in ΔG^{o} are accounted for by the T factor in Eq. (1).

2.2 Thermodynamic data from monitoring growth kinetics at steps

An atomic force microscopy (AFM) investigation (Feeling-Taylor *et al.*, 2001) revealed that similarly to many other inorganic and protein crystals (Giesen *et al.*, 1996; Malkin *et al.*, 1996; McPherson *et al.*, 2000; Yau *et al.*, 2000a; Yip & Ward, 1996), the crystals of HbC grow by a two step mechanism (a) a new layer is generated by a surface nucleation process; (b) these layers incorporate building blocks from the solution and spread to cover the whole facet, Figure 2.

Zooming on the edge of the growing layer, Figure 3, it was found that layer thickness equals ~ 55 Å and this is the molecular spacing in the **a** (or **b**) direction. Figure 3 shows that the edge of the unfinished layers is rough, and the characteristic lengthscale of the roughness equals one molecular dimension. This is only possible if molecules join the crystal one by one. We conclude that the building blocks of CO HbC crystals are single protein molecules.

Recording sequences of images such as the one in Figure 3 reveals that as the molecules attach to the edges of unfinished top crystal layers, these layers advance and the crystal grows. From Figure 3 and many other similar images, the following observations were made: (i) the number of molecules along the step edge between two kinks n_k varies between one and eight, with the mean $\bar{n}_k \approx 3$; (ii) comparing data collected at different supersaturation levels, we find that the mean does not depend noticeably on supersaturation.

Two mechanisms of generation kinks are discussed in literature. Gibbs suggested that in their thermal motion, molecules will be detaching and attaching themselves to the steps creating kinks (Gibbs, 1961). If the detachment energy of a molecule is too high and the kinks created by this mechanism are few and far apart, additional kinks may be generated by a "one-dimensional" nucleation process at elevated supersaturations (Chernov *et al.*, 1999). This second kink generation mechanism implies that the kink density will be a function of the supersaturation. Observation (ii) above allows us to conclude that the kinks are the result of thermal fluctuations of the step edge (Gibbs, 1961) and the kink density reflects the balance between the thermal energy of the molecules in

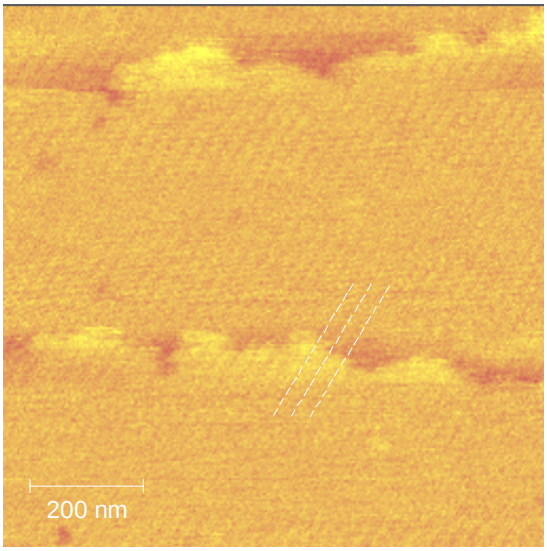

Figure 2
Spreading of growth layers on HbC crystals with each higher layer in perfect crystallographic alignment with the respective lower layer. White dashed lines highlight continuity between two layers of linear features in a ⟨010⟩ direction.

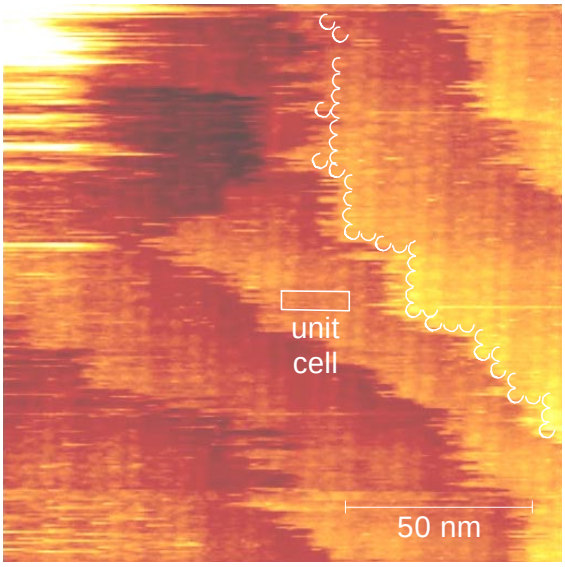

Figure 3
Molecular resolution image of the step edges during hemoglobin C crystallization. The crystallographic init cell and the molecules at the edge of one of the steps are highlighted..

the solution, and potential of interaction with their lattice neighbors in the crystal ϕ (Burton, 1951).

Because of the numerous associated water molecules, the interaction potential ϕ necessarily includes entropy components due to the release or trapping of the water molecules upon crystallization, as discussed above. Hence, ϕ should be viewed as a free energy, rather than as an enthalpy parameter. Exact accounting of the energetic and geometric factors yields the link between $\bar{n}_k$, the energy of kink formation w, and the free energy of intermolecular bond in the crystals ϕ (Burton, 1951)

$$\bar{n}_k = ½ \exp(w/k_BT) + 1 = ½ \exp(\phi/2k_BT) + 1. \quad (6)$$

Substituting the value of $\bar{n}_k$ for hemoglobin $\bar{n}_k \simeq 3$, Eq. (6) yields $\phi = 2.8\ k_BT = 7.0$ kJ mol^{-1}. The corresponding free energy of crystallization ΔG^o

$$\Delta G^o = -\phi Z/2 \quad (7)$$

where $Z = 6$ is the coordination number of a HbC molecule in a primitive tetragonal lattice. We get $\Delta G^o = -21$ kJ mol^{-1}.

Using Eq. (1), we can extrapolate the free energy values discussed above to 25 °C, the temperature of the AFM observations. We get $\Delta G^o \simeq -25$ kJ mol^{-1}. Compared to the value stemming from Eq. (5), we find that the value computed on the basis of the kink density is higher by 4 kJ mol^{-1}. This discrepancy could be due to the entropy loss of the protein molecules upon crystallization, $\Delta S^o_{protein}$ from Eq. (1). This entropy does not enter the determination based on Eq. (7), since this determination only accounts for pair interactions between the protein molecules. Comparing the two numbers for ΔG^o, we get $T\Delta S^o_{protein} \simeq -4$ kJ mol^{-1}, $\Delta S^o_{protein} \simeq -13$ J mol^{-1}K^{-1}. While the negative sign of $\Delta S^o_{protein}$ is easily understood in terms of the entropy loss due to the tying of the protein molecules, the magnitude of this parameter is significantly lower from some published values (Fersht, 1999; Page & Jencks, 1971). We attribute the low value of $\Delta S^o_{protein}$ to the contribution of the new vibrational degrees of freedom created upon the incorporation of a molecule, $\Delta S_{vibr} > 0$. If this ΔS_{vibr} is comparable in magnitude to the translational and rotational entropies of the free molecule in solution, lost upon incorporation, $\Delta S_{trans} + \Delta S_{rot} < 0$ (Tidor & Karplus, 1994), their sum $\Delta S^o_{protein} = \Delta S_{vibr} + \Delta S_{trans} + \Delta S_{rot}$ may by close to zero. Another possible explanation for the low $\Delta S^o_{protein}$ is that the chosen standard state, with its high protein concentration, has very low protein entropy and this masks the true entropy effect of a transfer of a protein molecule from the solution into the crystal.

An important point is that the choice of a standard state and the associated corrections in ΔG^o *do not affect* the following discussion of the entropy gain due to release of water in the thermodynamics of protein crystallization. As shown here, we can determine a $(\Delta G^o)' = \Delta G^o + T\,\Delta S^o_{protein} = \Delta H^o - T\,\Delta S^o_{solvent}$ from the statistics of the molecular configurations at steps. The determination of $(\Delta G^o)'$ is based on transfer of molecules between two states at the step and does not include the solution state, i.e., it is independent of the choice of the solution standard state. The values of $(\Delta G^o)'$ found from the step structure are close to those of ΔG^o discussed here. While this closeness raises questions about the dependence of the value of $\Delta S^o_{protein}$ on the choice of a solution standard state, it supports the fidelity of the values of $\Delta S^o_{solvent}$ discussed below.

2.3. The entropy gain due to release of water

The sign and the significant magnitude of ΔS^o indicate that the overwhelming component in the crystallization entropy of HbC is not due to the incorporation of the HbC molecules in the crystal, i.e., $\Delta S^o_{protein}$, which should be *negative*, but rather the one due to the release of water molecules attached to the Hb molecules in solution, $\Delta S^o_{solvent}$. Intermolecular attraction of large molecules, that arises when the structured water around hydrophobic patches at the surface becomes disordered as molecules are brought closer, has been called hydrophobic force (Israelachvili & Pashley, 1982; Tanford, 1980). From our data on hemoglobin, we cannot judge if the water molecules are adjacent to hydrophilic of hydrophobic surface patches. However, water structuring around hydrophilic patches is expected to lead to effective repulsion, see (Petsev *et al.*, 2000; Petsev & Vekilov, 2000). Hence, we assume that the above entropy gain, i.e., the free energy component that drives the molecules into

the crystal, is the hydrophobic interaction between the protein molecules (Eisenberg & Kauzmann, 1969; Eisenberg & Crothers, 1979; Tanford, 1961; 1980; Weber, 1991).

This conclusion allows us to crudely estimate the number of water molecules n_w released at the contact between two hemoglobin molecules. Since $\Delta S^o_{protein}$ is very small, $\Delta S^o_{solvent} \approx 600$ J mol^{-1}K^{-1}. Following an analogy first put forth by Tanford (Tanford, 1980), we compare the entropy effect of Hb crystallization to the entropy change for melting of ice, at 273 K, $\Delta S^o_{ice} = 22$ J mol^{-1} K^{-1} (Dunitz, 1994; Eisenberg & Kauzmann, 1969; Eisenberg & Crothers, 1979). This analogy is based on the fact that both in freezing and in binding to a protein molecule, water molecules are transferred from a relatively free and disordered state in the liquid, to a more ordered fixed-location state (Tanford, 1980). This analogy is supported by the estimates of the entropy loss due to the tying up of hydration water in crystals that have yielded 25 – 29 J mol^{-1} K^{-1} (Dunitz, 1994). Using these numbers, the above values of $\Delta S^o_{solvent}$ reflect the release of ~ 20-30 water molecules. With six molecules as nearest neighbors in the tetragonal crystal lattice (Perutz, 1969; Vasquez *et al*., 1998) and three intermolecular bonds per molecule in the crystal, this corresponds to the release of $n_w \approx 10$ water molecules per intermolecular bond.

3. Apoferritin – athermal crystallization driven by the release of water molecules

The solubility of apoferritin does not depend on temperature (Petsev *et al.*, 2001; Thomas *et al*., 1997). Determinations of the second virial coefficients of apoferritin were performed in the temperature range 15 to 35°C revealed no temperature dependence of the virial coefficient (Petsev *et al.*, 2001). This is in agreement with the correlation between the protein solubility correlates with the second virial coefficient discussed in (George & Wilson, 1994).

The lack of temperature dependencies of the solubility leads to the following physical conclusions: (i) the enthalpy of crystallization is zero (or extremely small), and (ii) the entropy of crystallization is independent of temperature. Conclusion (i) follows from Eq. (4) and $\partial C_e/\partial T = 0$. For conclusion (ii), we note that with $\Delta H = 0$, Eq. (2) becomes

$$\left(\frac{\partial \Delta G^o}{\partial T}\right) = \frac{\Delta G^o}{T} \qquad (8)$$

with a simple solution

$$\Delta G^o = const \times T,\ \Delta H^o = 0 \text{ and } \Delta S^o = const \qquad (9)$$

AFM monitoring of the behavior of monomolecular steps on the surface of an apoferritin crystal at 23 °C has yielded 23 μg cm^{-3} = 5.2×10^{-8} mol kg^{-1} (Yau *et al.*, 2000a; Yau *et al*., 2000b). Using Eq. (5), we get $\Delta G^o = -42$ kJ/mol. Note that in the case of apoferritin, the second, approximate equality in Eq. (5) converts to an exact relation. Light scattering determinations of the second virial coefficient of apoferritin in crystallizing solutions indicate an approximate balance between the repulsive and the attractive interactions, leading to a $\gamma \cong 1$ (Yau *et al*., 2000a). The closeness of ΔH^o to zero allows us to conclude that crystallization is mostly driven by the maximization of the entropy of the solvent. Applying Eq. (6.) to the structure of the steps during the growth of ferritin and apoferritin, illustrated in Figure 4, we get $\bar{n}_k = 3.5$. Then, $w = 1.6\ k_B T$. If we assume first-neighbor interactions only, the intermolecular bond energy, ϕ can be evaluated. In the face-centered cubic structure of the apoferritin crystals, when a molecule is moved from within the step on a (111) face to a location at the step, four kinks are created. For this, seven bonds (four in the top layer and three with molecules from the underlying layer) are broken, and five are formed. With $w = \phi/2$ and $\phi = 3.2\ k_B T \cong 7.8$ kJ/mol. With $Z_1 = 12$ for a fcc lattice, the standard free energy of formation of a single intermolecular bond in apoferritin crystals is – 7.0 kJ mol^{-1} (Yau *et al*., 2000b) and is fully attributable to the entropy gain due to the release of water (Yau *et al*., 2000a), i.e., the entropy effect per intermolecular bond is $\Delta S^o = 26.6$ J mol^{-1} K^{-1}. Comparing this value to ΔS^o_{ice}, as we did above for hemoglobin C, this corresponds to $n_w \approx 1$ or 2 for this protein.

This low number of water molecules can be tentatively linked to the structure of the intermolecular bonds in the face-centered cubic apoferritin crystals. The x-ray structure reveals that each of the twelve such bonds consists of a pair of Cd^{2+} ions (Lawson *et al.*, 1991). In each ion of the pair, 2 of the 6 coordination places

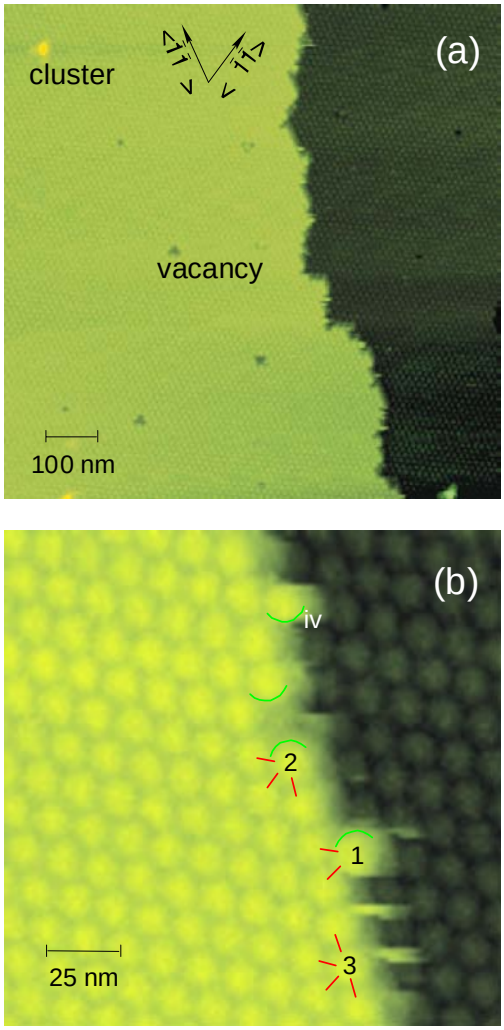

Figure 4
Molecular structures of a growth step on an apoferritin crystal at protein concentration of 70 μg/mL, corresponding to supersaturation $\sigma = 1.1$. Dark green: lower layer; yellow: advancing upper layer. (a) Lower resolution view. Adsorbed impurity clusters and surface vacancies are indicated. (b) Higher resolution view. Three different types of molecular positions at a step are marked with Arabic numbers, for details, see text. Bonds with molecules belonging to the top crystal layer are marked with red. Green arches and Roman numbers mark potential growth sites, "kinks".

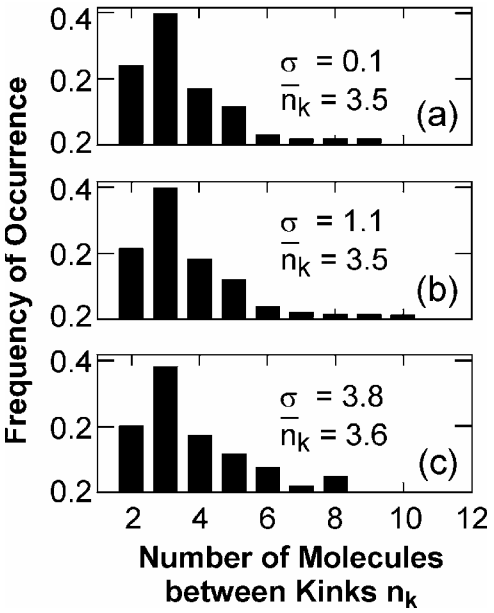

Figure 5
Distribution of number of molecules between kinks on steps of apoferritin crystals located > 0.5 μm apart, obtained from images similar to Figure 4a at the three supersaturations σ indicated in the plots, the mean values of the distributions for each case are also shown. The apoferritin concentrations corresponding to these σ's are a) 25 μg/mL, b) 70 μg/mL and c) 1 mg/mL.

are occupied by an aspartic acid residue from the one apoferritin molecule partaking in the bond and a glutamic acid residue from the other (Hempstead *et al.*, 1997). The fact that the entropy change corresponds to the release of one or two, rather than four water molecules suggests that the Cd^{2+} ions may be pre-bound to either the incoming apoferritin molecule, or to the apoferritin molecules already in the crystal.

Thus, as suggested by the crystal structures of ferritin and apoferritin (Harrison & Arosio, 1996; Hempstead *et al.*, 1997; Lawson *et al.*, 1991), the main component of the crystallization driving force stems for the strong Cd^{2+}-mediated bond between each pair of molecules. The unexpected part of our conclusion is that this driving force is not of enthalpy origin (the likely large negative enthalpy of such a bond must have been compensated for by unfavorable enthalpy effects of other patches of the molecules), but by the entropy of the water released during the formation of this bond.

4. Lysozyme – negative crystallization enthalpy and entropy

Over the last 15 years the solubility of lysozyme and in particular its tetragonal crystals has been studied by several groups, employing a variety of techniques (Ataka & Asai, 1988; Cacioppo *et al.*, 1991; Cacioppo & Pusey, 1991; Howard *et al.*, 1988; Miyashita *et al.*, 1993; Ries-Kautt & Ducruix, 1989; Rosenberger *et al.*, 1993). Fortunately, in the areas of overlap, these techniques have produced rather consistent results, certifying to the accuracy of the determinations (Miyashita *et al.*, 1993; Rosenberger *et al.*, 1993). In all cases, normal temperature dependence of the solubility was noted, indicative of negative crystallization enthalpy according to Eq. (4.). For several sets of conditions, the temperature dependencies of the solubility were used to determine the crystallization enthalpy, and different groups came up with values in the range of –72 to –80 kJ mol^{-1} (Ataka & Asai, 1988; Howard *et al.*, 1988). It appears that the enthalpy does not change much with variations in the crystallization conditions, at least within the range probed, and a direct calorimetric determination yielded a value of –75 kJ mol^{-1}, well within this range (Schall *et al.*, 1996).

Unfortunately, a complete thermodynamic analysis of the whole parameter space investigated in these studies is impossible because of the limited cross-section between the field of condition of the solubility data, and the respective field for the data on the second virial coefficient (Bonneté *et al.*, 1999; Guo *et al.*, 1999), required to evaluate the activity coefficient. We choose the set of conditions of 2.5 % (w/v) = 0.43 M NaCl in 0.05 M acetate buffer at pH 4.5. Solubility data for these conditions are available in the temperature interval from 12 to 32 °C (Rosenberger *et al.*, 1993). At the two ends, the solubility is 3.2 and 50 mg L^{-1}, respectively; the corresponding molalities are 0.0002 and 0.0029 mol kg^{-1}. The correction introduced by the activity coefficient for this protein is not negligible. Taking it into account and using the exact form of Eq. (5.), we get the free energy effect of crystallization at 12 °C, ΔG^o = –20 kJ mol^{-1}, and at 32 °C, ΔG^o = –15.6 kJ mol^{-1}. The crystallization enthalpy emerging from data in (Rosenberger *et al.*, 1993) is ΔH^o = –75 ± 3 kJ mol^{-1}. From Eq. (1.), the full entropy change during crystallization is ΔS^o = –193 J $mol^{-1}K^{-1}$, close to the ΔS^o = –210 J $mol^{-1}K^{-1}$ found for lysozyme crystallization in (Fersht, 1999; Finkelstein & Janin, 1989). The factor $T\Delta S^o$ = –54.8 kJ mol^{-1} at both temperatures, i.e., entropy is lost during crystallization, and the entropy change disfavors crystallization.

We can tentatively divide this entropy effect between $\Delta S^o_{protein}$ and $\Delta S^o_{solvent}$. One way to do this is by assuming $\Delta S^o_{protein}$ for lysozyme crystallization is insignificant, in analogy with the above findings for hemoglobin C and apoferritin. Then, $T\,\Delta S^o_{solvent} \approx -54$ kJ mol^{-1} and $\Delta S^o_{solvent} \approx -190$ J $mol^{-1}K^{-1}$. Scaling with the entropy of formation of ice, as introduced above for hemoglobin, we find that 8 or 9 water molecules are *trapped* in the crystal with the incorporation of each lysozyme molecule in addition to those associated with the molecule in the solution.

Acknowledgement

The conclusions of this work would have been significantly limited in scope and accuracy if not for the deep critical insight of A.A. Chernov. This work was supported by NHLBI, NIH through Grant HL58038; and NIH Minority PreDoctoral Fellowship Health 1F31 HL09564-01 to A.R.F.-T, the Office of Biological and Physical Research, NASA, through Grants NAG8-1354 and NAG8-1790.

References

Ataka, M. & Asai, M. (1988). *J. Crystal Growth*, **90**, 86-93.
Atkins, P. (1998). *Physical Chemistry*, 6th ed. Freeman, New York.
Bonneté, F., Finet, S. & Tardieu, A. (1999). *J. Crystal Growth*, **196**, 403-414.
Burton, W. K., Cabrera, N. &. Frank, F.C. (1951). *Phil. Trans. R. Soc. London Ser. A*, **243**, 299- 360.
Cacioppo, E., Munson, S. & Pusey, M. L. (1991). *J. Crystal Growth*, **110**, 66-71.
Cacioppo, E. & Pusey, M. L. (1991). *J. Crystal Growth*, **114**, 286-292.
Chernov, A. A., Rashkovich, L. N., Yamlinski, I. V. & Gvozdev, N. V. (1999). *J. Phys. Condens. Matter*, **11**, 9969-9984.
Dunitz, J. D. (1994). *Natur,e* **264**, 670-670.
Eaton, W. A., Munoz, V., Thompson, P. A., Chan, C. K. & Hofrichter, J. (1997). *Curr. Opin. Struct. Biol.* **7**, 10-4.
Eisenberg, D. & Kauzmann, W. (1969). *The structure and properties of water*. Oxford University Press.
Eisenberg, D. & Crothers, D. (1979). *Physical Chemistry with Applications to Life Sciences*. The Benjamin/Cummins, Menlo Park.
Feeling-Taylor, A. R., Banish, R. M., Hirsch, R. E. & Vekilov, P. G. (1999). *Rev. Sci. Instr.* **70**, 2845-2849.

Feeling-Taylor, A. R., Yau, S.-T., Hirsch, R. E., Nagel, R. & Vekilov, P. G. (2001). Submitted.
Fersht, A. (1999). *Structure and mechanism in protein science*, W.H. Freeman, New York.
Finkelstein, A. & Janin, J. (1989). *Protein Engineering* **3**, 1-10.
George, A. & Wilson, W. W. (1994). *Acta Cryst.* D**50**, 361-365.
Gibbs, J. W. (1961). *The Collected Works of J.W. Gibbs*, 1, Yale University Press, New Haven.
Giesen, M., Schulze Icking-Konert, G., Stapel, D. & Ibach, H. (1996). *Surf. Sci.* **366**, 229-238.
Guo, B., Kao, S., McDonald, H., Wilson, W. W., Asanov, A. & Combs, L. L. (1999). *J. Crystal Growth* **196**, 424-433.
Harrison, P. M. & Arosio, P. (1996). *Biochim. Biophys. Acta* **1275**, 161-203.
Hempstead, P. D., Yewdall, S. J., Fernie, A. R., Lawson, D. M., Artymiuk, P. J., Rice, D. W., Ford, G. C. & Harrison, P. M. (1997). *J. Mol. Biol* **268**, 424-448.
Hill, T. L. (1963). *Thermodynamics of small systems*, Benjamin, New York.
Howard, S. B., Twigg, P. J., Baird, J. K. & Meehan, E. J. (1988). *J. Crystal Growth* **90**, 94-104.
Israelachvili, J. & Pashley, R. (1982). *Nature* **300**, 341-342.
Israelachvili, J. N. (1995). *Intermolecular and Surface Forces*, Academic Press, New York.
Lawson, D. M., Artymiuk, P. J., Yewdall, S. J., Smith, J. M. A., Livingstone, J. C., Trefry, A., Luzzago, A., Levi, S., Arosio, P., Cesareni, G., Thomas, C. D., Shaw, W. V. & Harrison, P. M. (1991). *Nature* **349**, 541-544.
Malkin, A. J., Kuznetsov, Y. G., Land, T. A., DeYoreo, J. J. & McPherson, A. (1996). *Nature Struct. Biol.* **2**, 956-959.
McPherson, A. (1982). *Preparation and analysis of protein crystals*, Wiley, New York.
McPherson, A. (1999). *Crystallization of biological macromolecules*, Cold Spring Harbor Laboratory Press, Cold Spring Harbor New York.
McPherson, A., Malkin, A. J. & Kuznetsov, Y. G. (2000). *Ann. Rev. Biomol. Struct.* **20**, 361-410.
Miyashita, S., Komatsu, H. & Suzuki, Y. (1993). *Jap. J. Appl. Phys.* **32**, 1855-1857.
Page, M. I. & Jencks, W. P. (1971). *Proc. Natl. Acad. Sci.* **68**, 1678-1685.
Perutz, M. F. (1969). *Eur J Biochem* **8**, 445-66.
Petsev, D. N., Thomas, B. R., Yau, S.-T. & Vekilov, P. G. (2000). *Biophys. J.* **78**, 2060-2069.
Petsev, D. N. & Vekilov, P. G. (2000). *Phys. Rev. Lett.* **84**, 1339-1342.
Petsev, D. N., Thomas, B. R., Yau, S.-T., Tsekova, D., Nanev, C., Wilson, W. W. & Vekilov, P. G. (2001). *J. Crystal Growth*, **232**, 21-29.
Rariy, R. V. & Klibanov, A. M. (1997). *Proc. Natl. Acad. Sci. USA* **94**, 13520-13523.
Ries-Kautt, M. M. & Ducruix, A. F. (1989). *J. Biol. Chem.* **264**, 745-8.
Rosenberger, F., Howard, S. B., Sowers, J. W. & Nyce, T. A. (1993). *J. Crystal Growth*, **129**, 1-12.
Ross, P. D., Hofrichter, J. & Eaton, W. A. (1977). *J. Mol. Biol.* **115**, 111-134.
Ross, P. D. & Minton, A. P. (1977). *J. Mol. Biol.* **112**, 437-452.
Schall, C., Arnold, E. & Wiencek, J. M. (1996). *J. Crystal Growth* **165**.
Tanford, C. (1961). *Physical Chemistry of Macromolecules*, Wiley, New York.
Tanford, C. (1980). *The hydrophobic effect: formation of micelles and biological membranes*, John Wiley & Sons, New York.
Thomas, B. R., Carter, D. & Rosenberger, F. (1997). *J. Crystal Growth* **187**, 499- 510.
Tidor, B. & Karplus, M. (1994). *J. Mol. Biol.* **238**, 405-414.
Vasquez, G. B., Ji, X., Fronticelli, C. & Gilliland, G. L. (1998). *Acta Cryst.* D**54**, 355-366.
Weber, P. (1991). *Physical principles of protein crystallization*. In *Advances in protein chemistry* (Afinsen, C. B., Richards, F. M., Edsal, J. T. & Eisenberg, D. S., eds.), Vol. 41. Academic Press, New York.
Yau, S.-T., Petsev, D. N., Thomas, B. R. & Vekilov, P. G. (2000a). *J. Mol. Biol.* **303**, 667-678.
Yau, S.-T., Thomas, B. R. & Vekilov, P. G. (2000b). *Phys. Rev. Lett.* **85**, 353-356.
Yip, C. M. & Ward, M. D. (1996). *Biophys. J.* **71**, 1071-1078.

 Received 29 March 2002 • Accepted 7 August 2002